

# Digitally-modulated OOK Reconfigurable Intelligent Surfaces for Massively-scalable Gbps Transmitters

Himanshu Sharma<sup>(1)</sup>, Xiangbo Meng<sup>(1)</sup>, J Nicholas Laneman<sup>(1)</sup>, Ralf Bendlin<sup>(2)</sup>, Bertrand Hochwald<sup>(1)</sup>, and Jonathan Chisum<sup>(1)</sup>

<sup>(1)</sup> University of Notre Dame, IN 46556, USA, hsharma2@nd.edu, jchisum@nd.edu

<sup>(2)</sup> AT&T Labs, Austin, TX 78759, USA

**Abstract**—We present single-layer, direct digitally modulated, reconfigurable intelligent surface (RIS) unit-cell (UC) designs at 12GHz. These UCs find application in low-power, gigabits per second (Gbps) ON-OFF Keying (OOK) modulators where each UC of the surface can be individually programmed using Gbps general purpose input-output (GPIO) lines. The key challenge is to realize a large shift in response from a small voltage change (the direct digital drive). We propose that transmission efficiency  $\eta_T$  should be maximized and modulation depth  $m$  should be greater than 20 dB.

## I. INTRODUCTION

RISs are a promising technology for lowering the cost and energy required to deploy next-generation upper-mid-band (UMB) and millimeter-wave (MMW) networks [1]. They entail repetitive units of precisely tailored metal and substrate, called UCs having a tunable component. When modulated, they experience a change in their electromagnetic response. This paper focuses on design comparison of ultra-low complexity, direct-digitally driven, Gbps modulated RISs operating in the UMB, centered at 12 GHz. Unlike most RISs, wherein the state of adjacent UCs is correlated and their reconfiguration rate may be microseconds to milliseconds, each UC of the proposed surface will be individually modulated at Gbps speeds. In fast-switching applications, tunable UCs usually employ varactors, given their fast switching speeds (sub-ns) compared to PIN diodes. However, a large reverse bias voltage (0-5V) is necessary to induce a large change in capacitance, making direct digital drive impractical [2]. In order to support low-complexity, direct digital drive of massive sub-ns modulated surfaces, the UCs in this work maintain low-voltage modulation (350 mV) of varactors (see Fig. 1(e)). Thus, to induce a pronounced shift in reflection coefficient UCs employ high quality-factor embedding networks. In addition to direct digital drive, UCs should be low-complexity, simplifying manufacture for massive scaling. These challenges are addressed in the proposed UC designs below.

## II. DESIGN PROCEDURE AND SYMBOL ERROR RATE

The proposed RIS transmit cell is shown in Fig. 1(a): a local oscillator (LO) produces power at the RF carrier frequency (here, 12 GHz) using saturated, high-efficiency amplifiers. The RF signal propagates through an L-bend parallel plate waveguide (PPWG) (Fig. 1(b)) and is incident upon the RIS, a linear array of multiple UCs, on a 45° incline. Low-voltage differential signal (LVDS) baseband (BB) signals (Fig. 1(c)) modulate each UC of the RIS which individually modulate

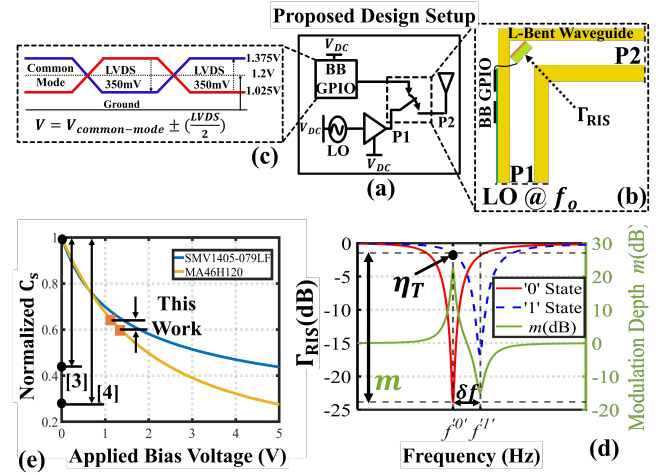


Fig. 1. Transmitter Design. (a) System model. (b) Side-view of the RIS in an L-Bent PPWG with input port P1 and radiating aperture P2. (c) BB GPIO control lines to modulate each UC. (d) Frequency response of a UC. (e) Capacitance-voltage relation for a typical varactor.

incident RF before being radiated from the exit aperture (Port P2). The LVDS levels are 1.375 V ( $V^1$ ) and 1.025 V ( $V^0$ ) in the “1” and “0”-states, respectively. This is a much smaller difference in levels than is typical (e.g., [3], [4] in Fig. 1(e)). The reflection coefficient of the RIS is a frequency-shifted resonance with a high (“1”-state) and low (“0”-state) reflection coefficient at 12 GHz to realizing OOK modulation. The response (Fig. 1(d)) depicts three figures of merit (FoM):

$$\text{Modulation Depth } m \text{ (dB)} \stackrel{\text{def}}{=} \Gamma_{RIS}^1 - \Gamma_{RIS}^0;$$

$$\text{Transmission Efficiency } \eta_T \text{ (\%)} \stackrel{\text{def}}{=} |\Gamma_{RIS}^1| \text{ at } f_o, \text{ and}$$

$$\text{Frequency Shift } \delta f \text{ (Hz)} \stackrel{\text{def}}{=} f^1 - f^0.$$

It is always advantageous to maximize transmission efficiency so we seek designs with high  $\eta_T$ . In order to determine the required modulation depth  $m$ , we derive the symbol error rate (SER) of a corresponding 1-bit OOK receiver [5] versus modulation depth of the proposed 1-bit OOK transmitter. Consider a discrete memory-less channel with received signal,

$$y = \text{sign}(x^2 - \psi + z), \quad (1)$$

where transmitted symbols  $x \in V_{LO}[\Gamma_{RIS}^1, \Gamma_{RIS}^0] = [x_1, x_0]$ ,  $\psi = \frac{x_1^2 + x_0^2}{2}$  is the 1-bit threshold, and  $z \sim \mathcal{N}(0, \sigma^2)$  is Normal distributed, zero mean back-end noise with variance  $\sigma^2$ . Applying maximum likelihood detection and a uniform distribution on  $x_1, x_0$ ,

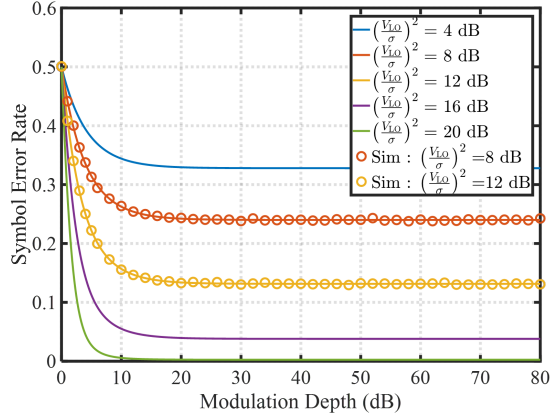


Fig. 2. SER versus modulation depth  $m$  for  $\eta_T = 75\%$ .

$$\hat{x} = \arg \max_{x \in \{x_1, x_0\}} P(y|x) = \begin{cases} x_0, & y < 0 \\ x_1, & y \geq 0 \end{cases} \quad (2)$$

with SER,

$$\text{SER} = Q \left( \frac{V_{LO}^2 \eta_T^2 (1 - \frac{1}{m^2})}{2\sigma} \right), \quad (3)$$

and  $Q$  being the probability of  $N(0, 1) > x$ . Figure 2 shows that SER saturates for all signal-to-noise ratios so we require UCs with  $m \geq 20$  dB.

### III. UNIT CELL TOPOLOGIES

This section compares the performance of several *single-layer*,  $\frac{\lambda}{2}$  ( $w, h = 12.5$  mm) UC topologies with ground planes in the back and the incident wave at 45°. A low-permittivity Rogers RT/Duroid 5880 substrate is used to reduce UC parasitic capacitance. Gbps OOK modulation with just 350 mV of change in bias voltage is achieved using a GaAs Flip-Chip Hyperabrupt varactor [MACOM MA46H120]. Using small signal analysis and operating far away from its device resonant frequency, the varactor is represented as  $R_s(V)$  and  $C_s(V)$  in the equivalent circuit models for UCs (Fig. 3). The RC values for the varactor in the “0” state are  $0.607 \Omega$  and  $0.822$  pF, respectively, while the corresponding values in the “1” state are  $0.577 \Omega$  and  $0.733$  pF. OOK modulation is achieved by producing a high-Q match (to free space,  $377 \Omega$ ) at  $f_0 = 12$  GHz, such that modulating the varactor substantially shifts the resonant frequency and results in a large modulation depth,  $m$ .

The simplest UC topology (Fig. 3(a)) has a single degree of freedom (DoF): substrate thickness  $t_{subs}$ . An equivalent parallel inductance  $L_1$  cannot, in general, match a particular varactor to  $377 \Omega$ . However, for the optimal varactor  $Q$ ,  $R_s(1+Q^2) = 377 \Omega$  and  $L_1$  will resonate out the capacitive reactance. This particular varactor cannot be matched with such a simple scheme at 12 GHz so  $\Gamma_{RIS} = 0$  dB and modulation depth is 0 dB. Further, due to the finite gap  $g = 0.7$  mm, there is a parasitic parallel capacitance,  $C_{UC}$  in the UC.

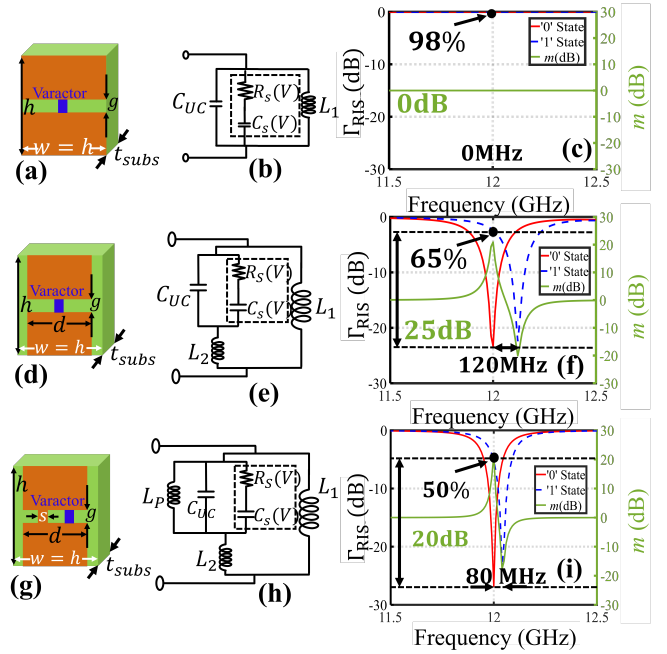


Fig. 3. UC topologies. Physical structure, equivalent circuit model and frequency response: (a)-(c) 1 DoF UC, (d)-(f) 2 DoF UC, (g)-(h) 3 DoF UC. Orange, green and blue represents 1-oz Cu, substrate and varactor.

Fig. 3(d) shows a UC with 2 DoF. The response (Fig. 3(f)), shows a match is obtained at  $f_0$  by changing Cu patch width  $d=7.5$  mm and substrate thickness  $t_{subs} = 15$  mil, to realize a series  $L_2$  and parallel  $L_1$ , respectively (Fig. 3(e)). Having 2 DoF allows the UC to be operated and matched at any frequency while maintaining fabrication limits. A better match at  $f_0$  with the same  $t_{subs}$  is realized by introducing a small Cu strip  $s = 0.25$  mm (Fig. 3(g)) to provide 3 DoF. This also provides for more robustness to fabrication tolerance. However, the FoMs reduce because, in order to match at  $f_0$ ,  $d=11$  mm which leads to an increase in  $C_{UC}$  and an overall lower net change in capacitance between “1” and “0”. As future work we will fabricate the 2 DoF UC and demonstrate its usefulness in a multi-cell RIS for OOK modulation.

This work was supported by AT&T Labs.

### REFERENCES

- [1] C. Pan et al., “Reconfigurable Intelligent Surfaces for 6G Systems: Principles, Applications, and Research Directions,” *IEEE Commun. Mag.*, v.59, n.6, pp.14-20, June 2021, doi: 10.1109/MCOM.001.2001076.
- [2] X. Chen et al., “Design and Implementation of MIMO Transmission Based on Dual-Polarized Reconfigurable Intelligent Surface,” in *IEEE Wireless Commun. Lett.*, v.10, n.10, pp. 2155-2159, Oct. 2021, doi: 10.1109/LWC.2021.3095172.
- [3] R. Fara, P. Ratajczak, D. -T. Phan-Huy, A. Ourir, M. Di Renzo and J. de Rosny, “A Prototype of Reconfigurable Intelligent Surface with Continuous Control of the Reflection Phase,” in *IEEE Wireless Communications*, vol. 29, no. 1, pp. 70-77, February 2022, doi: 10.1109/MWC.007.00345.
- [4] Liang J. C., et al., “An Optically Transparent Reconfigurable Intelligent Surface with Low Angular Sensitivity,” *Adv. Optical Mater.* 2022, 2202081. <https://doi.org/10.1002/adom.202202081>
- [5] N. J. Estes et al., “A 0.71-mW Antenna-Coupled On-Off-Key Receiver for Gbps Millimeter-Wave Wireless Communications,” in *IEEE Trans. Microw. Theory Techn.*, vol. 71, no. 4, pp. 1793-1808, April 2023, doi: 10.1109/TMTT.2022.3222424.